Optical Systems in Ultrafast Biophotonics

Pierre Laporte, Stéphane Ramstein, Stéphane Mottin
LTSI, CNRS UMR 5516,
F-42100 Saint-Etienne, France

Mottin@univ-st-etienne.fr
Mottin, S. identifier: http://orcid.org/0000-0002-7088-4353

http://doi.org/10.1117/12.514036
DOI DataCite : https://doi.org/10.5281/zenodo.439022

Reference BibTeX:

```
@article{2004_mottin_22,
TITLE = {Optical Systems in Ultrafast Biophotonics },
AUTHOR = { Laporte, Pierre and  Ramstein, Stéphane and  Mottin , Stéphane },
JOURNAL = {SPIE},
VOLUME = { 5249},
PAGES = { 490-500},
YEAR = {2004},
DOI = {10.1117/12.514036},
KEYWORDS = {Biophotonics;Optical systems;Second-harmonic generation;Streak camera;Optoelectronics;Photonics;Time-resolved
spectroscopy;femtosecond laser;streak camera;in vivo monitoring;brain;neurophysiology;FADH;milk;water;fluorescence},
}
```

ABSTRACT

In the field of biophotonics the main goals are the control and processing of *in vivo* biological tissues and the monitoring of biomolecule dynamics. Two particular “pitfalls” are present: the dynamic multiscale organization and the photostress of the medium. Until now the state of the art of the pico-femtosecond systems designed to these applications shows that the changing laser technology has been only used as an add-on. Our approach is based on a bottom-up procedure and on the medium-centered knowledge. The range of neurobiological applications of ultrafast photonics extends from TRP (time-resolved propagation) to linear and non-linear TRE (time-resolved emission).

The device combines a one kilohertz chirp pulse amplification laser system and a single shot streak camera. For discrete wavelength applications (TRE), the set-up is a SHG/OPG/OPA^3/SHG design. In the case of TRP, the beam is focused into pure water to generate a white light continuum. After propagation through tissue, a single-shot streak camera with single photo-electron counting capability performs the picosecond time-resolved spectroscopy of the collected photons. Depending on the acceptable level of photostress, the integration time can extend from 33ms up to several minutes with a real-time control of the jitter and time drifts.

The meaning of the TRE spectro-temporal image is particularly detailed in the 450-480nm excitation window in regards to the contributions of mitochondrial flavoproteins.

This optical system fulfills the reliability and the sensitivity, conditions required for measuring opto-electronic quantities from freely moving animal at low irradiation.

Keywords: Time-resolved spectroscopy, femtosecond laser, streak camera, *in vivo* monitoring, brain, neurophysiology, FADH, milk, water, fluorescence.

1. INTRODUCTION

Design optimization of a system means the modification of the structure and the parameters to minimize the total levelized cost of the apparatus under conditions associated with available materials together with the safety, reliability, operability and maintainability of the system. Optics technology and applications related to biomedical research and health care are a special case of optical system design. Biophotonics, the science of light in life sciences, has a history of success in solving clinical, biological and research problems in diverse applications through such products and techniques as microscopy, imaging, spectroscopy and fiber optics. One of the main particular trouble is the complexity of the medium. Moreover in the water spectral window from 200nm to 1000nm, the medium interacts with light via many photobiochemical and photobiomechanical pathways. To overcome these specific “pitfalls” (complexity and regulated photoactions), the optical system must reach the reliability and the sensitivity of the measured opto-electronic quantities at low irradiation.

 Contact: mottin@univ-st-etienne.fr Identifier http://orcid.org/0000-0002-7088-4353

Our efforts are focused on the monitoring of the activity of the grey nucleus or the cerebral cortex in freely moving or anaesthetised rodents and birds by optical methods. The understanding of the interactions between light and these tissues needs complex optical designs in order to obtain consistent measurable quantities.
A fundamental principle underlying analysis and design is to consider complex systems (here the whole optical system &medium) as interconnected (linear or no linear) blocks with signals being conveyed between them, and modified by passage through the blocks. There are many levels of understanding possible in such a framework, and they are obtained by using tools such as differential equation modeling, Laplace transform analysis and impulse/harmonic response...
With these tools it is well established that the use of constant signals is not sufficient to avoid artefact in complex system measurements. To get the optical transfer function of the target (mainly chromophores in tissue), the design of the instrument must get the best experimental responses to typical optical inputs: the Dirac delta function, the unit step input or the Heaviside's function, the ramp input and the sinusoidal input (or other periodic signals). In this paper we focus on the proper use of the optical "near Dirac delta function". The photo-electronic response comes up to the transfer function.
In order to investigate the complex biological media like nervous tissue, two domains of optical techniques appear:

(1) time-resolved propagation (TRP)
(2) time-resolved emission (TRE) with linear and non-linear emissions, in particular fluorescence.

1.1. Time-resolved propagation (TRP)

Since the pioneering work[1], neurometabolic coupling and neurovascular coupling have been studied by picosecond light transillumination. Visible and NIR spectral window could probe cerebral perfusion, oxygenation (saturation level) and the distribution of brain absorbers[2]. But until now, a reliable neuromethod based on intrinsic optical signals remains a challenge due to the multifaceted aspects of tissue optics.
Intrinsic optical absorption has been less studied in regards to its heterogeneous spatial distribution. Homogenization of the heterogeneous absorption has been considered with basic phantoms[3,4,5]. Van Veen and Sterenberg[6] described effective coefficient approaches to quantify the difference in absorption between homogeneously distributed and discrete distribution of blood. Many theoretical approaches have been presented to determine absorption changes in different compartments of a layered structure (homogeneous absorption coefficient in each layer) from spatial profiles of time-integrated intensity and mean time of flight[7] or from time and space-resolved mapping[8].
Brain could be described as a multi-scale porous medium in regards to photonic absorption (porous volume corresponds to non-absorbing volume). In the NIR window, absorption mainly depends of the distribution of red blood cells enclosed within discrete vessels with tissue specific angio-architecture. With injected exogenous chromophore the molecular distribution is limited to the whole vascular volume.
In time-resolved measurements, the *in vivo* "averaged absorption" is often quantified with a limited number of wavelengths. Many optical instrumental designs (steady-sate, pulse, harmonic...) have been proposed: multi-point detectors and multi-point emitters. But until now, any of them has been approved for routine clinical use, i.e. Advanced Research Technologies Inc. is in the process of bringing to market SoftScan®, a digital imaging device which uses this Company's time domain optical imaging technology to detect and diagnose breast cancer. The first results of the pre-clinical trial with McGill University were announced in June 26, 2003. And they are contrasted. One of the main recurrent limit is the use of few discrete wavelengths or in the case of steady-state apparatus, the lack of time-of-flight.
We propose a new imaging solution for the direct measurements of chromophore (i.e. hemoglobins, flavins) or for the reliable detection of cancer (i.e. heterogeneity in absorbers concentration) without the adverse consequences associated with traditional technology. To get a wide spectral window with time-resolved measurements, an optical system is designed: a real-time broadband time-resolved spectroscopy where femtosecond white light continuum generation is combined with streak camera technology. And to minimize photostress, the streak camera works in single photo-electron counting mode.
White light continuum was first observed by Alfano and Shapiro[9]. When the intensity reaches 10^{14}-10^{15} W/mm^2, the beam undergoes self-focusing with many no linear phenomena[10]. The beam breaks up into small filaments, while the spectrum of each filament increases until the radiation becomes white. Continuum is a very interesting source for ultrafast spectroscopy[11]. At high frequency, nJ pulses from a femtosecond oscillator can also induce continuum generation in tapered fibres[12]. The analysis of these optical systems designs leads to distinguish four domains: low repetition rate (<1kHz), —middle (1-100 kHz) , —high (100kHz-1MHz), —very high repetition rate (>1MHz). The optimization of the ratio counting rates/(thermal and chemical stress) is not easy. The very high repetition rate needs synchroscan streak camera. The repetition rate below 1MHz implies a laser with amplification stages. But the single shot streak camera tolerates many flexible and open modes. After the supercontinuum generation, its propagation is quantified by a streak camera. Many developments of streak camera technology occur in the field of ultra-speed photography with different trigger modes[13]. The first white light continuum time-resolved spectroscopy designed to tissue optics[14] was at a low

repetition rate (10Hz). For medical and biological studies, two drawbacks of this low repetition rate could be underlined: 1) high energy per pulse, 2) time of measurement above five minutes. The kHz design with chirped pulse amplification can easily perform different qualities of the supercontinuum. Other instrumental design could be discussed in the range of KHz to hundred MHz repetition rates. A kHz design is under patent protection[15]. The differential time-resolved spectrophotometry by SPE counting with white light generation is also under patent protection[16].

Theory

The diffusion approximation is a well established basic approach in tissue optics[17,8]. The partial differential equation is the following heat equation:

$$\left[\frac{\partial}{\partial t} - D\,c\,\nabla^2 + \mu_a c\right]\left(\varphi(r,t)\right) = S_0(r,t)$$

c is the group velocity equal to the speed of light (0.3mm/ps) divided by the averaged refraction index of the medium (n=1.4). μ_a is the absorption coefficient in mm^{-1}. $D = (3(\mu_a+\mu_s'))^{-1}$. μ_s' is the reduced scattering coefficient in mm^{-1}. μ_s' is usually far greater than μ_a. "*D* c" is the homogenized coefficient of diffusivity in mm^2/ps. $\varphi(\mathbf{r},t)$ is the photon density (number of photons/mm^3 or J/mm^3). $\varphi(\mathbf{r},t)$ could be the fluence (J/(s mm^2) and S_0 must be homogeneous to a fluence.

In the nIR window, the tissue absorption spectrum ($\mu_a = f(\lambda)$) mainly depends of the distribution of hemoglobins. If absorption properties could be homogenized then the solution is (in infinite medium (R^3) and with S_0 = spatial et temporal Dirac delta function):

U(t) is the Heaviside's function.

$$\varphi(r,t) = U(t)\frac{\exp(-r^2/(4Dct) - \mu_a c t)}{\pi^{3/2}(4Dct)^{3/2}}$$

This equation represents the shape of the output signal measured under ideal conditions, i.e. with an infinitely short pulse, a detection system with an instantaneous response, and with a spatial delta function at contacts with the volume probed. The measured signal S(t) is the convolution of the transfer function with the instrument response function.

The photonic diffusion coefficient (Dc) is in the range of 0.02mm^2/ps. The Fourier time is defined by $t_F = L^2/(4Dc)$. At the end the fundamental dimensionless quantity is t/t_F .

In the case of typical length of propagation (10mm), picosecond time scale is required. By comparison with mass transfer, i.e. oxygen in water at 37°C, the study needs a time scale of few seconds. (diffusion coefficient ≈ 0.03mm^2/(10s)). By comparison with heat transfer in tissue, the study needs a time scale of few hundred milliseconds (typical tissue thermal conductivity without blood circulation is equal to 0.015mm^2/(100ms)).

We use the solution of the diffusion equation with proper photonic boundary conditions published by Patterson et al[18].

If the signal shape is far less of this symbolic function, the need of tissue anatomy increases the difficulty of averaging chromophore concentration. The detection of absorbers heterogeneities is a complex task. In this paper we only focus on averaged absorption coefficient.

1.2. Time-resolved emission (TRE)

TRE systems are mostly optical molecular imaging devices to help pharmaceutical companies and research laboratories to better understand physiology and physio-pathology and reduce the development cycle for new drugs.

Here we present the assessment of fluorescence occurring in the 500-600 nm window in a deep brain nucleus of freely moving animals.

Why time-resolved analysis is so important in biophotonics, especially in fluorescence? It is well known that the use of constant signals, steady-state fluorescence, is not sufficient to avoid artefact in biochemometry[19]. In tissue optics, time-resolved fluorescence allows a control of quantum efficiency stability or fluctuation and other parameters which lead to reliability[20].

Another step of tissue optics in freely moving animal could be imaging system[21,22]. But the meaning and the reliability of "one pixel" autofluorescence signal must be achieved. Does time-resolved spectroscopy allow a reliable link between the target (chromophore concentration, chromophore dynamics) and opto-electronic signals? Consistent answers[23] imply a complex optical design.

Either in TRP and in TRE applications, the real-time spectro-temporal approach is a robust way[16,23] to get an "optical identity card" and a trustworthy relation between chemometry and photonics signals in the case of complex turbid media.

 Contact: mottin@univ-st-etienne.fr Identifier http://orcid.org/0000-0002-7088-4353

2. MATERIALS AND METHODS

2.1. The setup

The figure 1 presents the experimental setup. The laser system is composed of a mode-locked oscillator (Coherent, Mira or Vitesse, 760-840nm) and a chirp pulse amplification laser system (BMI-Thalès Alpha 1000). After the compression stage, this system produces 170 fs pulses (FWHM measured by autocorrelation) with 0.5 mJ/pulse at 1 kHz.
After the chirp pulse amplification laser system, two systems are designed : — for TRE, an OPG/OPA system, — for TRP, a white-light generation.
For discrete wavelength applications, mainly TRE, the set-up is a SHG/OPG/OPA^3/SHG (SHG : second harmonic generation, OPG: optical parametric generator, OPA : optical parametric amplifier; all crystals are BBO) and succeeds in generating tunable UV-vis-nIR down to 230nm with more than 2 hours stability. The full tunable window is :

Design	excitation wavelength	available power
SHG/OPG/OPA^3/SHG	230nm-370nm,	>1.5 mW
SHG	375 nm-410nm,	>150mW
SHG/OPG/OPA^3	425nm-700nm,	> 60mW (in nIR, with the idler).

In the case of real-time TRP, the pump beam is focused (focal length equal to 21 cm) into pure water to generate a white light continuum (450nm-950nm) with a power of more than 100mW with several hours stability. After continuum generation, a spatial filter composed by a circular diaphragm is used for removing the purple/blue ring of conical emission. Two fibres (0.3m length, numerical aperture 0.4, core diameter equal to 0.4mm) are at the calculated positions on the calvaria according to the Paxinos atlas[24] in order to probe visual cortex, somato-sensory cortex or motor cortex. After propagation through tissues, the light is dispersed by a polychromator (270M, Spex Jobin-Yvon). A single-shot streak camera (Hamamatsu Streakscope C4334) with single photo-electron counting capability[25], triggered with a fast photodiode, performs the picosecond time-resolved spectroscopy of the collected photons. The spectral window width is 176 nm, according to the applications. The streak camera allows photoelectron detection with 2 ps time resolution per pixel and a full range of 1.127 ns. The typical one shot streakscope function response given by Hamamatsu is 14ps (FWHM). Each frame of the streak camera integrates 33 laser pulses.
Depending on the acceptable level of photostress, the integration time can extend from 33ms up to several minutes. This wide range of accumulation time needs a real-time control of the jitter and the time drift. The data processing of the spectro-temporal images is a key step either for TRE and TRP.

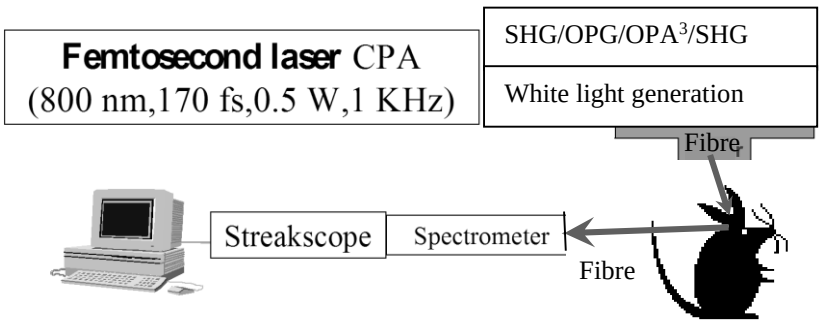

Fig 1: Optical systems design for tunable or broadband spectral time-resolved spectroscopy.
Two optical fibres are used in TRP (Øcore=0.4mm). One optical fibre is used in TRE (Øcore=0.2mm).

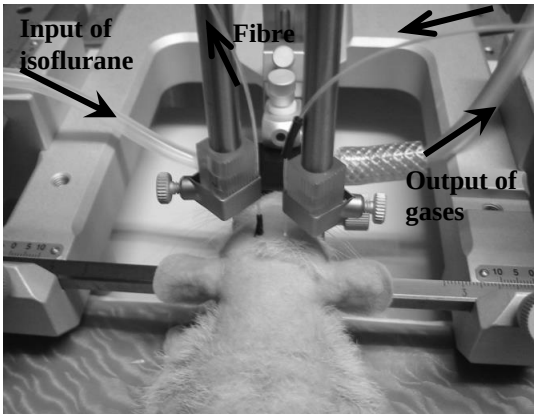

Fig 2: TRP with anaesthetized rat preparation. Under stereotaxic conditions. An interhemispheric measurement is illustrated.

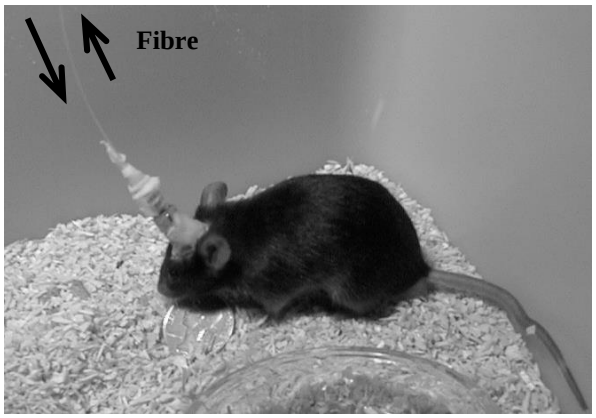

Fig 3: TRE with freely moving rodent (here a mouse). In the case of rat, two cannula on the head could be used.

2.2. Animal preparation

The figure 2 and the figure 3 illustrate the animal preparations.

For TRP experiments, male hairless Sprague-Dawley rats (350-400 g b.w., OFA-hr/hr, Charles River, Italy) are anaesthetized with isoflurane under stereotaxic conditions (Stoelting Co., USA) in order to achieve the best precision for the optical fibre positions and the neuro-anatomical conditions. The distance between the source fibre and the detection fibre is set to 5 mm. In this paper the cortical area investigated is the M2 motor cortex.
In the case of TRE experiments, the freely moving animal preparation was previously published[20,23].

3. RESULTS AND DISCUSSION

3.1. TRP

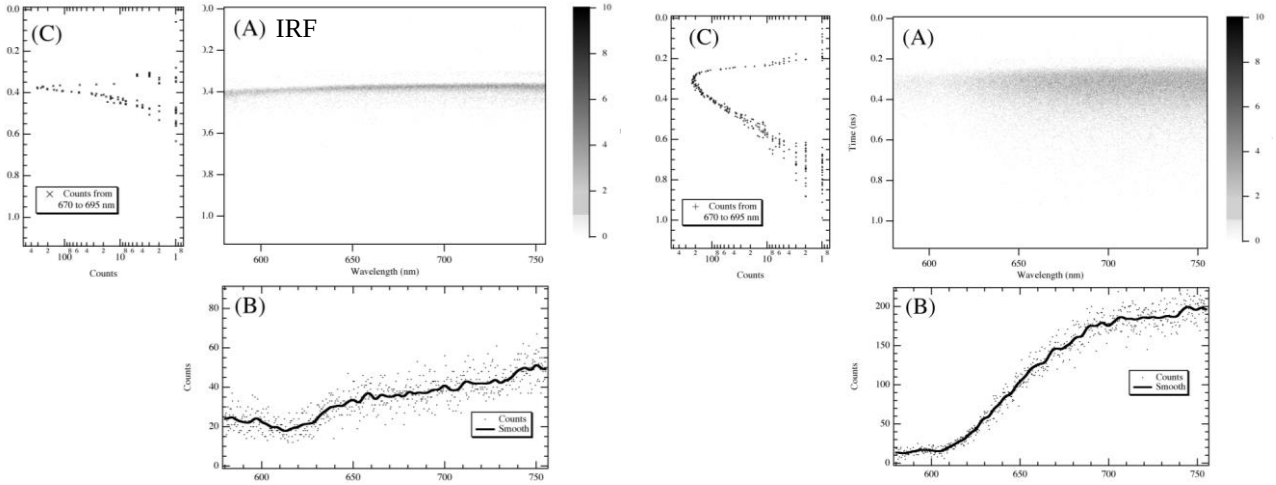

Fig 4: A typical time-resolved spectroscopy image of the instrumental response function (IRF) and derived from the dorsal rat head transillumination. The grey levels of the Z-axis give the number of SPE counts (single photoelectron: SPE) for each pixel. Grey becomes darker throughout the SPE counting. The spectrum is shown in part B. The figure C is the temporal shape of the spectral window 670-695nm.

The figure 4 shows the instrumental response function and the results from *in vivo* rat head transillumination. This time-resolved spectral image results from 25000 laser shots with a 1000Hz triggering signal. Here the wavelength window extends from 580nm to 756nm. The spectra (fig4-B) are uncorrected (no filter to flatten the spectrum, no correction of the spectral sensitivity of the photocathode). The temporal shape of the spectral window 670-695nm is shown in the part C of the figure 4. The full width at half maximum (FWHM) of the IRF reaches 30ps.
For the time-resolved spectroscopy image derived from the dorsal rat head transillumination (right hemisphere), the distance between the white-light continuum and the optical fibre is 7mm. This image gives you an idea about these tissues are highly scattering and absorbing media. This figure clearly shows that below 620nm, the *in vivo* absorption coefficient is too high with our geometry (7mm). Comparisons with published data[26] show a large difference between 670nm and 633nm. These differences on the absorption coefficient are expected due to the high increase of hemoglobin extinction coefficient in this range. The relative decrease of the counting rate between 750nm and 620nm of the *in vivo* spectra is in the range of 600%. Below 620nm, even at high distances (≥10mm), time-resolved spectroscopic image presents residual SPE counts with short time-of-flight. The light transillumination method implies penetration and collection at the skull surface. Photons enter in the vascular and trabecular structures of calvaria (in rat 500-700µm depth). Due to the special trabecular structures, this layer presents a complex photon migration. After this bony surface, light reaches meningis and cortical structures. The residual SPE counts below 620nm could come from a skull layer effect.
For a distance of 7mm and below 620nm, the *in vivo* absorption coefficient is too high and stops from doing a sufficient counting rate to get a reliable measurement. So the final choice is to set the window to 660nm. The geometry is put to the "inter-distance limit" which is equal to 5mm. In this case, classic theoretical calculus with homogenate medium hypothesis shows that the cortical layers are the most probable region probed. The investigation of layered media is one of the first steps for the resolution of neurovascular probing. If it is well established that the two homogenate layers problem is nearly solved[27], it remains a challenge to give accurate answers to the following question in neurophotonics: where are photons killed by using the measurement of the photon survivors?

The validation of the full system (experimental setup and spectro-temporal image analysis methods) has been performed with a simple model widely used in tissue optics, the semi-skimmed UHT milk. The figure 5 compares results measured with our design for Indian ink diluted in semi-skimmed milk and Indian ink diluted into pure water (*same concentration measured with a steady-state spectrophotometer*). The quantitative spectra are in agreement (see figure 5).

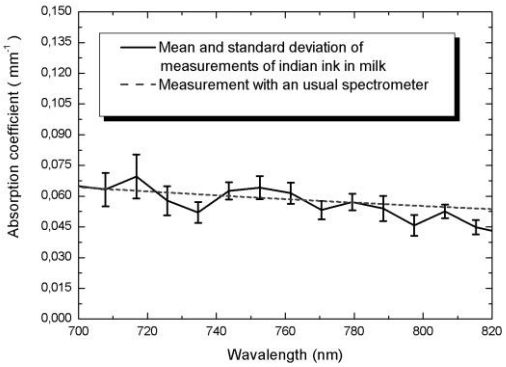

Fig 5: Absorption spectra for Indian ink diluted into semi-skimmed milk with our setup and for Indian ink diluted into pure water with a steady-state spectrophotometer.

With the distance between the source fibre and the detection fibre is equal to 5 mm, the analysis of the rat brain transillumination spectro-temporal images leads to the figure 6. In the spectral window from 660 nm to 810 nm, the spectra of four repeated measurements, their mean and standard deviation show the apparent homogenate scattering and absorption coefficients. The absorption coefficient extends from 0.075 mm^{-1} to 0.040 mm^{-1}. Scattering is flat and the μ_s' is around 4.3 mm^{-1} for this spectral window.

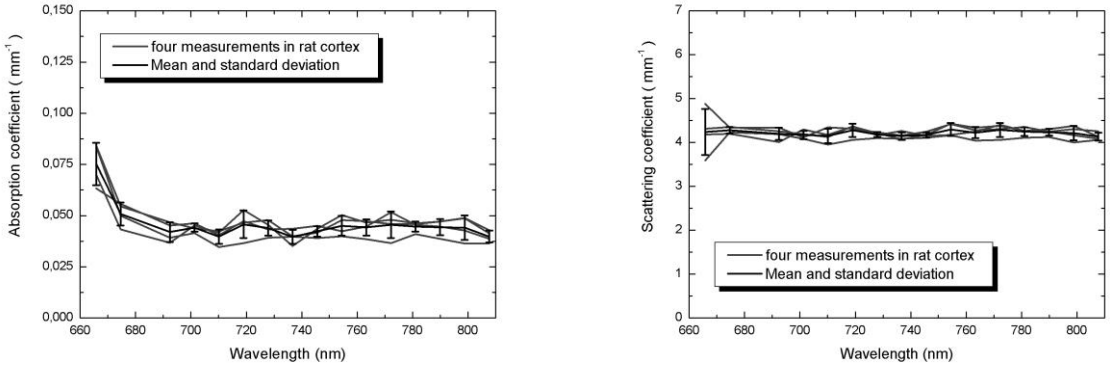

Fig. 6 Absorption and scattering spectra by *in vivo* time-resolved rat brain femtosecond white-light transillumination

In neurobiology, the potential of this kilohertz method is that short pulses at visible and nIR wavelengths can be used for probing the complex superficial neurovasculature without excision of a portion of the skull and with a 25s time of measurement. With this integration time, the instrumental response function allows a 30ps resolution. The conversion efficiency {800nm->window of interest} remains limited to around 22% in our design without focal spot optimization (wavefront correction) and without optimizing the medium with salts and ions.

3.2. TRE

Some TRE results were published in the case of the excitation between 337nm and 355nm[23]. The link between intramitochondrial NADH and TRE image has been detailed[23]. In this paper, some results in the "flavin spectral window" (excitation wavelength window 450-475nm) are described.

The figure 7 illustrates the time-resolved emission spectroscopy of the Raphe Nucleus in the freely moving rat. The complexity of a such image needs other images acquired from more basic media.

The figure 8 shows the spectro-temporal image of a limpid FADH solution in saline solution (20µM).

The figure 9 is the spectro-temporal image of semi-skimmed milk with an half dilution with saline solution in order to get similar scattering properties and flavins autofluorescence.

The spectro-temporal image is shown at part A. The spectral shape and the temporal shape are respectively the part B and the part C.The excitation is performed at 450nm with 0.2mW at the tip of the optical fibre. In the case of figures 7 to 9, the acquisition time is respectively 90s, 360s and 100s in order to get the range of one hundred counts for the peak value of the temporal shape (550-565nm spectral window).

The emission peaks near 550nm with different spectra and different decay-times.

In regards to optical systems design research, one of the main problem with this design is the residual level in the emission spectral window. Due to a high scattering coefficient and the one optical fibre design, the signal is in competition with the back-scattering of the femtosecond parametric source. If the excitation is tuned to 475nm without moving the spectral window of the polychromator, this backscattering prevents the measurement. An optimized dichroïc mirror could reduce this noise. A definitive solution is to turn the source to picosecond pulse by reducing the spectrum in the stretcher and modifying the stretcher/compressor lengths and also the crystal lengths. With these changes and at 1ps, the tunability range is reduced, the fluctuation is twice more and the UV power is only 30% of the femtosecond value. Depending on the application and the spectroscopy requirements, the choice extends from 150fs to 1ps.

In regards to biological analysis of these results, it is evident that this excitation spectral window needs new researches in particular involving the genetically encodable fluorophores (GFP, green fluorescent protein and its variants)[28]. It is not easy to see GFP in the sea of other fluorescent compounds in the cell. This cerebral endogenous autofluorescence is not only a "noise" but also a complex molecular signal! When animals are killed with a lethal dose of anesthetic, the apparent autofluorescence always decreases (results not shown). In the case of NADH autofluorescence, the signal increases[20].

Tissue optics studies have grown dramatically for the last ten years, particularly in brain optics[29]. Mainly four phenomena have been "under the light": absorption , fluorescence, scattering and photo-acoustic. Spontaneous emission in tissue is a phenomenon where absorption and scattering play a major role. So interpretation of tissue fluorescence needs careful biophotonic analysis in order to link photo-electron signals to biological events and quantitative data. For this goal time-resolved emission spectroscopy is well suited in the field of *in vivo* neuro-energetics[23]. Acquiring in real-time both spectral data and temporal shapes allows decorrelation of the effects of molecular absorptions, inner filters and complex tissue scattering (vascular compartments, extracellular compartments, etc...). The fluorescence analysis in high scattering media is also an old hot topic in biophotonics[30]. More and more biologists want to join molecular assessment to fluorescence. They expect linear regression between photonic signals and concentration in a definite domain, which depends on whole animal or tissue and or cellular models.

The green autofluorescence might rely on mitochondrial oxidised flavins. Previous studies investigating flavin fluorescence used an excitation peak at 460 nm, eliciting a fluorescent peak at 560-580 nm[31,32]

Chung et al.[33] showed that cerebral cortex of rat exhibits two fluorescence peaks at 520 and 630 nm, corresponding to excitation at 440 and 490 nm, respectively, and they assume that the most likely fluorophores potentially representing these two peaks are flavin and porphyrin respectively. Scholtz et al.[34] have shown that more than 90 % of the tissue flavin fluorescence change is due to mitochondrial flavoproteins. Rat mitochondrial enzymes present numerous different enzyme-bound flavin[35]. Mitochondrial flavin fluorescence originates on the basis of different optical and electrochemical properties from three oxidized flavoproteins[36]: the NAD-dependent a-lipoamide dehydrogenase, the CoQ-dependent electron-transfer flavoprotein and a fraction exclusively reducible by dithionite, the latter fraction may correspond to cytochrome b5 reductase, a flavoprotein of the outer membrane of the mitochondria. Contributions of other mitochondrial flavoproteins to the overall flavin fluorescence signal can be neglected[35]. Moreover, in rat brain mitochondria, the spectrum of some electron-transfer flavoprotein is almost absent[36]. Then, green autofluorescence of rat brain could come from the NAD-dependent a-lipoamide dehydrogenase and the fraction exclusively reducible by dithionite. The perspective is to precise the origins of this endogeneous emission by neuropharmacological drugs.

 Contact: mottin@univ-st-etienne.fr Identifier http://orcid.org/0000-0002-7088-4353

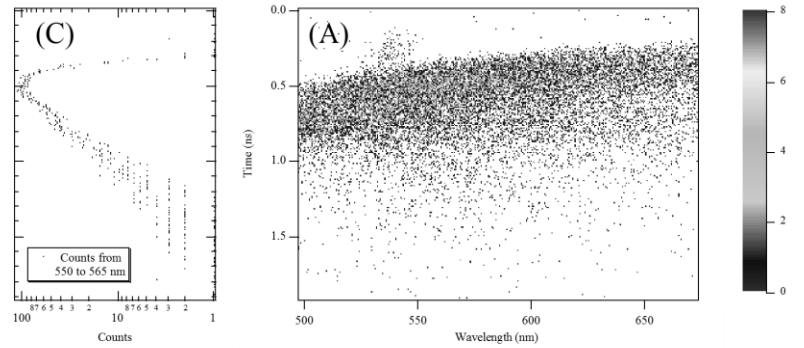

Fig. 7: The spectro-temporal image of the raphe nucleus autofluorescence under 450nm excitation wavelength with freely moving rat preparation.

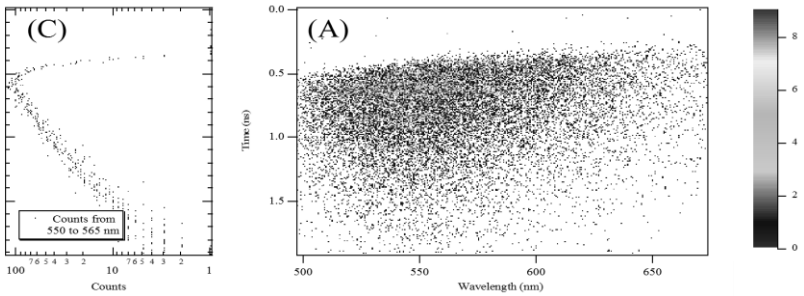

Fig. 8: The spectro-temporal image of a FADH 20µM solution under 450nm excitation wavelength

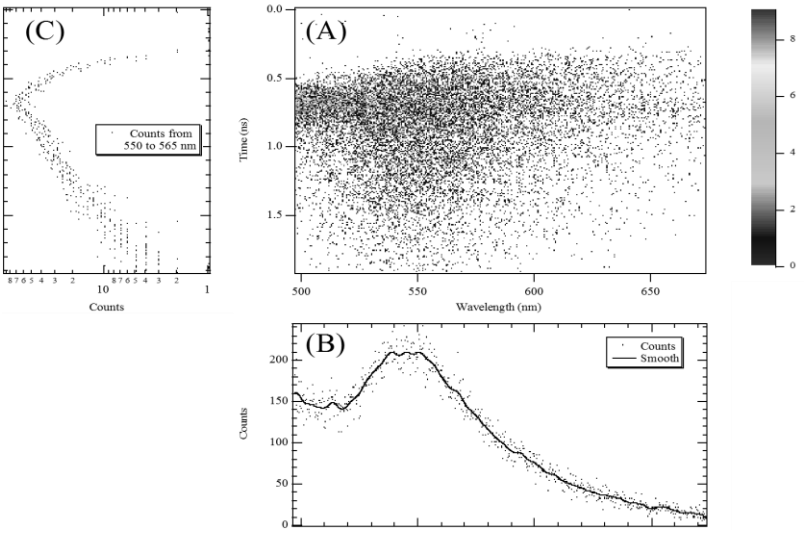

Fig. 9: The spectro-temporal image of the semi-skimmed milk autofluorescence under 450nm excitation wavelength. The semi-skimmed UHT milk is half diluted by saline solution.

Considering that only the oxidized forms of the flavins are fluorescent[36], the intrinsic autofluorescence signal from flavoprotein in the mitochondrial respiratory chain may be used to detect changes in the oxygen supply-demand ratio[37]. Based on steady-state spectroscopy and histology, this bibliographic analysis of the link between green autofluorescence signal and the tissue distributions of flavoproteins opens the door to the complexity of biophotonics.
Based on time-resolved fluorescence, it is well known that even in "quiet" limpid solutions, photophysical properties of flavoproteins are also complex[38]. *In vitro* free or bound-flavins quantum efficiencies are very sensitive. It is beyond this article to discuss the complex free- and bound-flavins photophysics but with our *in vivo* method, we have observed no significant temporal shape and fluorescence decay-time variations under stimili (results not shown).
The use of the fluorescence under two photon absorption could be an interesting next step.
At the end the brain flavin autofluorescence signal may be closely related to cellular metabolic activity[33]. The next step is the two photon imaging to a depth of 1mm in living brain[39].

4. CONCLUSION

4.1. TRP

The TRP design is reliable for the measurement of absorption spectrum in highly scattering media as semi-skimmed UHT milk. Measurements in rat motor cortical area need a more complex analysis. For *in vivo* studies, between the injection fibre and the collection fibre set to 5 mm, the range of $<\mu_a>$ and $<\mu_s'>$ as function of the wavelength reported in this work falls within the usual range, respectively 0.040-0.075 mm^{-1} and 4.3 mm^{-1} for the 660–810 nm spectral window. By comparison with extinction coefficient of hemoglobins, a range of the concentrations of oxygenated and deoxygenated hemoglobin could be deduced from these time-resolved measurements Real time monitoring down to one second, is the next step for this defy.

4.2. TRE

Rapid assessment of the metabolic changes occurring within defined brain regions of unanesthesied animals with a 0.2 mm spatial resolution which correspond to nuclei dimension, and sub-second resolution, is of wide interest for neurobiologists to link behaviour and neurophysiology. The deal is to allow identification and real-time following of interesting neuromolecules. Research in ultrafast biophotonic systems design will help this challenge.
To our knowledge, the method and the optical design reported here are the first ones allowing identification and following of "flavins" in deep brain tissue of unanaesthetized rats, and potentially of any freely moving vertebrate. $FAD/FADH_2$ turnover measurement, together with the assessment of NADH variations, constitutes an outstanding tool to explore brain metabolic changes *in vivo* in relation with behaviour.

ACKNOWLEDGMENTS

The authors wish to thank M[lle] Clémentine Vignal, Pr. Raymond Cespuglio and Dr.Nicolas Mathevon.

REFERENCES

1. Delpy D. T., Cope M., Van der Zee P., Arridge S., Wray S. and Wyatt J., "Estimation of optical pathlength through tissue from direct time of flight measurement", *Phys. Med. Biol.,* **33** (12), pp. 1433-1442, 1988.
2. Villringer A. and Chance B., "Non-invasive optical spectroscopy and imaging of human brain function", *Trends Neurosci.,* **20** pp. 435-442, 1997.
3. Liu H., Chance B., Hielscher A. H., Jacques S. L. and Tittel F. K., "Influence of blood vessels on the measurement of hemoglobin oxygenation as determined by time-resolved reflectance spectroscopy", *Med. Phys.,* **22** (8), pp. 1209-1217, 1995.
4. Firbank M., Okada E. and Delpy D. T., "Investigation of the effect of discrete absorbers upon the measurement of blood volume with near-infrared spectroscopy", *Phys. Med. Biol.,* **42** pp. 465-477, 1997.
5. Lohwasser R. and Soelkner G., "Experimental and theoretical laser-Doppler frequency spectra of a tissuelike model of a human head with capillaries", *App. Opt.,* **38** (10), pp. 2129-2137, 1999.
6. van Veen R. L. P. and Sterenborg H. J. C. M., *"Correction for inhomogeneously distributed absorbers in spatially resolved diffuse reflectance spectroscopy"*, Proc. SPIE 4431, S. Andersson-Engels and M. F. Kaschke, pp. 192-194, 2001.
7. Steinbrink J., Wabnitz H., Obrig H., Villringer A. and Rinneberg H., "Determining changes in NIR absorption using a layered model of the human head", *Phys. Med. Biol.,* **46** (3), pp. 879-896, 2001.
8. Avrillier S., Tinet E., Tualle J. M., Prat J. and Ettori D., *"Propagation d'impulsions ultracourtes dans les milieux diffusants. Application au diagnostic medical"*, Systèmes femtosecondes, Ed. P. Laporte, F. Salin and S. Mottin, Publications de l'Université de Saint-Etienne, pp. 295-310, 2001.
9. Alfano R. R. and Shapiro S. L., "Emission in the region 4000 to 7000 angstrom via four-photon coupling in glass", *Phys. Rev. Lett.,* **24** pp. 584-587, 1970.
10. Brodeur A. and Chin S. L., "Ultrafast white-light continuum generation and self-focusing in transparent condensed media", *J. Opt. Soc. Am. B,* **16** (4), pp. 637-650, 1999.
11. Pommeret S., van der Meulen P., Buntix G., Naskrecki R. and Mialock J.-C., *"Artefacts dans une expérience pompe-sonde"*, Systèmes femtosecondes, P. Laporte, F. Salin and S. Mottin, Publications de l'université de Saint-Etienne, pp. 183-207, 2001.
12. Birks T. A., Wadsworth W. J. and Russel P. S. J., "Supercontinuum generation in tapered fibres", *Opt. Lett.,* **25** (19), pp. 1415-1417, 2000.
13. Kieffer J.C. "*technologies de camera à balayage de fente femtoseconde"*, Systèmes femtosecondes, P. Laporte, F. Salin and S. Mottin, Publications de l'université de Saint-Etienne, pp. 269-280, 2001.
14. Andersson-Engels S., Berg R., Persson A. and Svanberg S., "Multispectral tissue characterization with time-resolved detection of diffusely scatterd white light", *Opt. Lett.,* **18** (20), pp. 1697-1699, 1993.
15. FOLESTAD, Staffan, JOSEFSON, Mats, SPARON, Anders, JOHANSSON, Jonas; 2001-03-29 ;WO0122063A1; ASTRAZENECA AB.
16. MOTTIN Stéphane, french patent under PCT; UJM CNRS.
17. Ishimaru A., "*Wave propagation and scattering in random media"*, NewYork, 1978
18. Kienle A. and Patterson M. S., "Improved solutions of the steady state and the time-resolved diffusion equations for reflectance from a semi-infinite turbid medium", *J. Opt. Soc. Am. A,* **14** pp. 246-254, 1997.
19. MOTTIN, S. TRAN-MINH, C., LAPORTE, P., CESPUGLIO R. and JOUVET M., Fiber optic time-resolved fluorescence sensor for *in vitro* serotonin determination, Applied Spectroscopy **47**, pp. 590-597, 1993,
20. MOTTIN, S., LAPORTE, P., CESPUGLIO R. and JOUVET M., Determination of NADH in the rat brain during sleep wake states with an optic fibre sensor and time resolved fluorescence procedures, Neuroscience, **79**, pp. 683-693, 1997
21. Helmchen F, Fee MS, Tank DW, Denk W., A miniature head-mounted two-photon microscope. high-resolution brain imaging in freely moving animals. Neuron **31**, pp. 903-912 , 2001.
22. Yoder E. J., Kleinfeld D. Cortical Imaging Through the Intact Mouse Skull Using Two-Photon Excitation Laser Scanning Microscopy, MICROSCOPY RESEARCH AND TECHNIQUE **56**, pp. 304–305, 2002.
23.Mottin S, Laporte P, Cespuglio R. Inhibition of NADH oxidation by chloramphenicol in the freely moving rat measured by picosecond time-resolved emission spectroscopy. J. Neurochem. **84** (4), pp. 633-642, 2003.
24. Paxinos G. and Watson C., "*The rat Brain in stereotaxic coordinates Third Edition"*, 1997.
25. Watanabe M., Koishi M., Fujiwara M., Takeshita T. and Cieslik W., "Development of a new fluorescence decay measurement system using two-dimensional single-photon counting", *J. Photochem. Photobiol. A: Chem,* **80** pp. 429-432, 1994.

26. Bevilacqua F. (1998). Local optical characterization of biological tissues in vitro and in vivo. Thesis n°1781, Ecole Polytechnique Fédérale de Lausanne.
27. Tualle, J.M., Tinet, E., Avrillier, S. "*Mesure des coefficients optiques dans des milieux diffusants stratifiés*", Signaux et milieux complexes, Publications de l'Université de Saint-Etienne, pp. 89-99, 2002.
28. Billinton N. and Knight. A. W., Seeing the Wood Through the Trees: A Review of Techniques for Distinguishing Green Fluorescent Protein from Endogenous Autofluorescence. *Analytical Biochemistry.* **291**, pp. 175-197, 2001.
29. Villringer, A. and Chance, B. Non-invasive optical spectroscopy and imaging of human brain function. *Trends Neurosci.* **20,** pp. 435-442, 1997.
30. Chang J., Graber, H., Barbour R. Luminescence optical tomography of dense scattering media, JOSA A, **14**,1, pp. 288-297, 1997.
31. Mayevsky A. Brain energy metabolism of the conscious rat exposed to various physiological and pathological situations. *Brain Research* **113**, pp. 327-338, 1976.
32. Chance B, Schoener B, Oshino R, Itshak F and Nakase Y. Oxidation-reduction ratio studies of mitochondria in freeze-trapped samples. NADH and flavoprotein fluorescence signals. *J.Biol.Chem.* **254**, pp. 4764-4771, 1979.
33. Chung YO, Schwartz JA, Gardner CM, Sawaya RE and Jacques SL. Diagnostic potential of laser-induced autofluorescence emission in brain tissue. *J Korean Med Sci.* **12**, pp. 135-142, 1997.
34. Scholtz R, Thurman RG, Williamson JR, Chance B and Bücher Th. *J.Biol.Chem.* **244**, pp. 2317-2324, 1969.
35. Kunz WS and Kunz W. Contribution of different enzymes to flavoprotein fluorescence of isolated rat liver mitochondria. *Biochim.Biophys.Acta* **841**, pp. 237-246, 1985.
36. Kunz WS and Gellerich FN. Quantification of the content of fluorescent flavoproteins in mitochondria from liver, kidney cortex, skeletal muscle, and brain. *Biochem Med Metab Biol.* **50**, pp. 103-110, 1993.
37. Barlow CH, Harden WR, Harken AH, Simson MB, Haselgrove JC, Chance B, O'Connor M and Austin G. Fluorescence mapping of mitochrondrial redox changes in heart and brain. *Crit Care Med.* **7**, pp. 402-406, 1979.
38. Wolfbeis, O. S.and Schulman, S. G. "*The fluorescence of organic natural products*" in Molecular Luminescence Spectroscopy, method and applications: Part 1; New-York; Wiley J. & sons, **77**, pp. 167-370, 1985.
39. Theer P, Hasan MT, Denk W. Two-photon imaging to a depth of 1000 microm in living brains by use of a Ti:Al2O3 regenerative amplifier. *Opt Lett.* **28**, pp. 1022-4, 2003.